Osteogenesis induced by frizzled-related protein (FRZB) is linked to the netrin-like domain

Sarah Thysen[1], Frederic Cailotto [1], Rik Lories [1,2]

[1] Laboratory of Tissue Homeostasis and Disease, Skeletal Biology and Engineering Research Center, Department of Development and Regeneration, KU Leuven, Belgium
[2] Division of Rheumatology, University Hospitals Leuven, Belgium

Corresponding author: Dr. Rik Lories, Laboratory of Tissue Homeostasis and Disease, SBE Research Centre, O&N1 – Box 813, Herestraat 49, B3000 Leuven, Belgium. Rik.Lories@uz.kuleuven.be. Phone: +32-16-342541; Fax: + 32-16-342543.

Running title: *SFRPs and osteogenesis*

Grant numbers and sources of support: This work was supported by an OT ("Onderzoekstoelage") grant from KU Leuven and by FWO-Vlaanderen (Flanders Research Foundation), grants G.0470.10 and G.0A42.13.

ABSTRACT

Abnormal Wnt signaling is associated with bone mass disorders (Westendorf J. et al., 2004). Frizzled related protein (FRZB, also known as secreted frizzled-related protein-3 (*SFRP3*)) is a Wnt modulator that contains an amino-terminal cysteine-rich (CRD) domain and a carboxy-terminal Netrin-like (NTN) motif (Cruciat C., et al., 2013). *Frzb*$^{-/-}$ mice show increased cortical thickness (Lories R., et al., 2007). However, the direct effect of FRZB on osteogenic differentiation and the involvement of the structural domains herein is not fully understood. In this study, we observed that stable overexpression of *Frzb* in MC3T3-E1 cells increased calcium deposition and osteoblast markers compared to control. Western blot analysis showed that the increased osteogenesis was associated with reduced canonical, but increased non-canonical Wnt signaling. On the contrary, loss of *Frzb* induced the opposite effects on osteogenesis and Wnt signaling. To translationally validate the positive effects of FRZB on primary human cells, we treated human periosteal and human bone marrow stromal cells with conditionned medium from MC3T3-E1 cells overexpressing *Frzb* and observed an increase in Alizarin red staining. We further studied the effect of the domains. $Frzb_{NTN}$ overexpression induced similar effects on osteogenesis as full length *Frzb*, whereas $Frzb_{CRD}$ overexpressing cells mimicked loss of *Frzb* experiments. The CRD domain is considered the Wnt binding domain, but the NTN domain also has important effects on bone biology. FRZB and other SFRPs or their specific domains may hold surprising potential as therapeutics for bone and joint disorders considering that excess of SFRPs has effects that are not expected under physiological, endogenous expression conditions.

***List of abbreviations*:**

alkaline phosphatase (ALP); antibiotic- antimycotic (AB); calcium-calmodulin-dependent kinase II (CamKII); conditioned medium (CM); cysteine-rich domain (CRD); Frizzled (Fz); Frizzled related protein (FRZB); human bone marrow stromal cells (hBMSCs); hypoxanthine guanine phosphoribosyl

transferase1 (Hprt1); human periosteum-derived cells (hPDCs); Netrin-like (NTN); secreted frizzled related protein (SFRP); tissue inhibitors of metallo-proteinases (TIMPs); type I procollagen C-proteinase enhancer proteins (PCOLCEs)

The Wnt signaling pathway is a key regulator of development, tissue growth, homeostasis and disease. Animal models and human genetic syndromes link abnormal Wnt signaling with high and low bone mass (1, 2). The Wnt family is a large group of lipid-modified secreted glycoproteins. Mammals have 19 Wnt homologs composed of 350 to 400 amino acids that share an *N*-terminal signal sequence for secretion followed by a nearly invariant pattern of 22-24 cysteines and several *N*-glycosylation sites (3, 4). Wnts are palmytoylated intracellularly by the enzyme porcupine. The presence of the lipid side chain affects solubility and signaling range.

Active Wnt signaling typically involves the canonical or β-catenin dependent cascade. In the absence of Wnt ligand, Frizzled (Fz) receptor and low-density lipoprotein receptor-related protein-5/6 coreceptor interaction, β-catenin is caught in a molecular destruction complex, phosphorylated and degraded by the proteasome. Upon Wnt-receptor interaction, the destruction complex is tethered away towards the receptor complex or disassembles, β-catenin accumulates in the cell, translocates to the nucleus and associates with transcription factors of the T-cell factor/lymphoid enhancer factor family. Wnts also signal through β-catenin-independent pathways. The planar cell polarity pathway activates GTPases of the RHO family and c-Jun N-terminal kinase to regulate the cytoskeleton and cell polarity, while the Wnt/Ca^{2+} pathway stimulates heterotrimeric G proteins, intracellular calcium release and activation of various calcium-sensitive enzymes such as protein kinase C, calcium-calmodulin-dependent kinase II (CamKII) and phosphatase calcineurin (3, 5).

The secreted frizzled related protein (SFRP) -family comprises five secreted molecules (SFRP1-5) and can modulate both canonical and non-canonical Wnt cascades. Every SFRP contains an amino-terminal cysteine-rich (CRD) domain and a carboxy-terminal Netrin-like (NTN) motif. The CRD domain shares structural homology with the Fz receptor and is therefore considered the Wnt binding domain. The NTN domain shows homology to the axonal guidance protein Netrin and is also found in tissue inhibitors of metallo-proteinases (TIMPs), complement proteins and type I procollagen C-proteinase enhancer proteins

(PCOLCEs). Until now, the exact role of the NTN domain in SFRP function remains unclear (6, 7).

SFPRs were originally identified as extracellular ligand-binding inhibitors of the Wnt signaling cascade. Recent data suggest that SFRPs have a broad range of biological activities, including negative and positive modulation of Wnt signaling (8, 9) and interactions with molecules unrelated to Wnt signaling (7). Deletions of *Frizzled-related protein (Frzb (Sfrp3))* in mice leads to increased cortical thickness without changes in the trabecular bone (10). Here, we aimed to directly assess the effect of FRZB on osteogenic differentiation and to elucidate the involvement of the CRD and NTN domain. .

MATERIALS AND METHODS

Molecular constructs

The pcDNA3.1-full length *Frzb*, pcDNA3.1- *Frzb* Δ $CRD_{\text{AA39-145 (7C)}}$ (referred to as Frzb_{NTN}) and pcDNA3.1-*Frzb* Δ $NTN_{\text{AA160-316}}$ (referred to as Frzb_{CRD}) constructs were earlier described (11).

Cell culture

Human periosteum-derived cells (hPDCs) and hBMSCs (a kind gift from C. Verfaillie, KU Leuven) were isolated as described earlier (12, 13). HPDCs, hBMSCs and MC3T3-E1 cells were cultured in maintenance medium DMEM (Gibco, Merelbeke, Belgium) containing 10% fetal bovine serum (FBS, Gibco), 1% antibiotic-antimycotic (AB, Invitrogen, Merelbeke, Belgium) and 1% sodium pyruvate (SP, Invitrogen).

Generation of stably transfected MC3T3-E1 cell lines

MC3T3-E1 cells were transfected with control pcDNA3.1+, pcDNA3.1-*Frzb*, pcDNA3.1-$Frzb_{CRD}$ or pcDNA3.1-$Frzb_{NTN}$ constructs using lipid-based agent Fugene HD (Roche Diagnostic, Vilvoorde, Belgium). Selection was initiated 24 hours after transfection by supplementing the maintenance medium

with 0.1 mg/ml geneticin (Invitrogen) for pcDNA3.1-$Frzb_{CRD}$ and 1 mg/ml for all other constructs. Clones were picked after 14 days of selection. Three different antibiotic-resistant clonal colonies of each condition were isolated and grown independently. Overexpression levels were assessed by quantitative RT-PCR (Q-PCR). Silencing of *Frzb* was performed using a pGIPZ-shmiRNA construct directed against mouse *Frzb* (Thermo Scientific, Aalst, Belgium) and a non-interfering pGIPZ vector (Thermo Scientific) was used as control. MC3T3-E1 cells were transfected using Arrest-In transfection reagent (Thermo Scientific) and after 24 hours, seletion with 1 µg/ml puromycin (Invitrogen) was initiated and continued for 7 days. Three different antibiotic-resistant clonal colonies of each condition were isolated and grown independently. Knockdown efficiency was assessed by Q-PCR. Antibiotic pressure was maintained for the whole duration of the experiments.

Osteogenic differentiation

Stably transfected MC3T3-E1 cells were seeded at 2.5 x 10^4 cells/well in 6-well culture plates (Thermo Scientific) in maintenance medium. At day 1, medium was changed to differentiation medium (α-Minimum Essential Medium Eagle (α-MEM) (Gibco) containing 10% FBS, 1% AB, 10 mM β-glycerophosphate and 50 µg/ml L-ascorbic acid-2-phosphate). The medium was refreshed every other day for 21 days. HPDCs were seeded at 1.5 x 10^4cells/well in 12-well culture plates (Thermo Scientific, Nunc) in maintenance medium. At day 1, medium was changed to differentiation medium consisting of α-MEM supplemented with 10% FBS, 1% AB, 10 mM β-glycerophosphate, 50 µg/ml L-ascorbic acid-2-phosphate and 0.1 nM dexamethasone (Sigma-Aldrich, Bornem, Belgium). Medium was changed every other day for 28 days of differentiation. Cells were stored at different time points for Alizarin red staining, RNA, protein extraction and alkaline phosphatase (ALP) activity assay. All conditions were performed in triplicate. For competition experiments with recombinant mFrzb, the differentiation medium was supplemented with 100 ng/ml recombinant mFrzb (RnD systems) for 14 days. For experiments under the stimulation of canonical or non-canonical Wnts, we treated the MC3T3-E1 cells with 100 ng/ml recombinant mWnt3a (RnD systems) or mWnt5a (RnD systems) during 14 days of differentiation.

Conditioned medium (CM) experiment

Supernatant (referred to as CM) was harvested every other day from confluent T75 culture flasks of MC3T3-E1 cells stably transfected with pcDNA3.1+ control vector or pcDNA3.1-*Frzb*. The supernatant was cleared by centrifugation at 3500 rpm for 10 min, and supplemented with 10 mM β-glycerophosphate and 50 µg/ml L-ascorbic acid-2-phosphate. Cells stably transfected with pcDNA3.1+ were seeded and the medium was refreshed every other day with differentiation medium enriched with supplemented CM in a 2:1 v/v ratio. At day 1 and 21 cells were stored for Alizarin red staining and ALP activity assay. For hPDCs and hBMSCs differentiation with CM, the medium was refreshed every other day with differentiation medium enriched with supplemented CM derived from MC3T3-E1 cells stably transfected with pcDNA3.1+ control vector or pcDNA3.1-*Frzb*. The supernatant was cleared by centrifugation at 3 500 rpm for 10 min and supplemented with 10 mM β-glycerophosphate, 50 µg/ml L-ascorbic acid-2-phosphate and 0.1 nM dexamethasone. The medium was refreshed every other day with differentiation medium enriched with supplemented CM in a 2:1 v/v ratio. At day 1 and 28 cells were stored for Alizarin red staining. Each condition was performed in triplicate.

Western blot analysis

MC3T3-E1 cells were harvested and resuspended in 0.05% Triton X (AppliChem, Zedelgem, Belgium) in PBS (Lonza, Verviers, Belgium) supplemented with 1 mM phenylmethanesulfonyl (Sigma-Aldrich), 5% protease inhibitor cocktail (Sigma-Aldrich), 2.3 mM Na_3VO_4 (Sigma-Aldrich) and 5 mM NaF (Merck Millipore, Overijse, Belgium). Cell lysates were sonicated (2 cycles of 7 s) and centrifuged at 13 000 rpm for 10 min, followed by protein quantification using the Pierce BCA Protein Assay kit (Thermo Scientific). A total of 7.5 µg of protein of each sample was denatured and separated on a 4-12% polyacrylamide Bis-Tris gel (Invitrogen) by electrophoresis using NuPage MES SDS Running buffer (Invitrogen). Proteins were transferred to a PVDF membrane (Merck Millipore). Non-specific binding sites were blocked using 5% non-fat milk in Tris-buffered saline with 0.1% Tween (Applichem) (TBS/T)

for one hour at room temperature. Primary antibodies were incubated overnight at 4°C with the following antibodies: 1/1 000 active- (dephosphorylated) β-catenin (CTNNB1) mouse antibody (Millipore), 1/1 000 total β -catenin mouse antibody (BD Biosciences, Aalst, Belgium), 1/1 000 anti- pCamK rabbit antibody (Cell Signaling Technology, Leiden, The Netherlands), 1/1 000 anti-CamK (pan) rabbit antibody (Cell Signaling Technology), 1/1000 anti-pCREB antibody (Cell Signaling Technology), 1/1000 anti-CREB antibody (Cell Signaling Technology) and 1/7500 anti-actin rabbit antibody (housekeeping gene; Sigma-Aldrich) in 5% bovine serum albumin in TBS/T (Cell Signaling Technology). Secondary horseradish peroxidase -conjugated antibodies were added and blots were developed using SuperSignal West Femto Maximum Sensitivy Substrate (Pierce, Thermo Scientific). Densitometry of blots was performed using Image J software (version 1.46r, National Institutes of Health) (Supplementary Table 1 and 2).

qPCR

Total RNA was isolated using NucleoSpin RNAII kit (Machery-Nagel, Düren, Germany) following the manufacturer's protocol. Complementary DNA was synthesized from 0.5-1 μg of total RNA using the RevertAid H minus First Strand cDNA synthesis kit (Fermentas GmbH, Rockford, IL USA). The SYBRgreen master mix system (Fermentas GmbH) was used to verify differential expression of *bFrzb, mFrzb, Osterix, Osteocalcin* and *Axin2* (Table 1). SYBRgreen quantitative analysis was performed on the Corbett Rotor-Gene 6000 (Corbett Research, Westburg, Leusden, The Netherlands) as follows: 10 minutes at 95°C, 40 cycles of 15 seconds of denaturation at 95°C, followed by 60 seconds of annealing-extension at 60°C. Melting curve analysis was performed to ensure amplification of a specific product. Results are expressed using the comparative threshold method (14) and normalised to housekeeping gene *Hprt1* (hypoxanthine guanine phosphoribosyl transferase1).

ALP activity

Cells were resuspended in 0.05% Triton X in PBS and sonicated (2 cycles of 7 s). ALP activity was measured using the BluePhos® Microwell Phosphatase Substrate System (KPL, Gaithersburg, Maryland

USA) following the manufacturer's instructions. Absorbance was measured at 495nm with a Titertek Plus MS212 microplate reader (Tecan, Mechelen, Belgium). When absorbance reached the saturation level, samples were diluted 1 in 3 in 0.05% Triton X in PBS.

Alizarin red staining and quantification

At day 1, 7, 14 and 21, cells were washed with PBS and fixed with ice cold 95% methanol for 30 min. Next, cells were washed with water and stained with 1% Alizarin Red (Sigma-Aldrich) at pH 4.1-4.3 for 10-15 min. 3 washing steps with water removed the unbound staining solution. Stains were dissolved in 10% acetic acid for 30 min. Cells were scraped off the culture plates, vortexed and heated for 10 min at 85°C. After 5 min on ice, the solution was centrifuged at 13 000 rpm for 15 min at 4°C. 10% ammonium hydroxide was added to the aqueous phase in a 1:5 v/v ratio. Absorbance was measured at 405nm with a Biotek Synergy HT microplate reader. When absorbance reached the saturation level, samples were diluted 1 in 3 in a mixture of 10% acetic acid and 10% ammonium hydroxide (1:5 v/v ratio). The mineralization nodules in the hPDCS and hBSMCs CM experiments were quantified using Image J software (NIH).

Statistics

Data were analyzed by 2-way ANOVA taking into account repeated measurements as observations over time could not be considered independent. Time *and Frzb* expression were defined as factors. The overall effect of both factors and their interaction was evaluated. Post-hoc Sidak tests were applied for the different time-points when interaction between time and target gene expression was found. Alpha was set at 0.05.

RESULTS

Overexpression of Frzb increases osteogenesis

We studied the effects of FRZB on differentiation and mineralization in MC3T3-E1 cells, a mouse calvarial osteoblast precursor cell line. Stably transfected MC3T3-E1 cells were used and high expression levels of *Frzb* were sustained throughout the 21-day experiments (average fold increase compared to control $3.5*10^3$) (Figure 1A). Overexpression of *Frzb* resulted in significantly enhanced Alizarin red staining (2-way ANOVA $p < 0.0001$ for interaction between time and *Frzb* overexpression – $p < 0.05$ between control and overexpression at day 14 and 21, but not day 1 and 7, with difference between means respectively -4.8 (95%CI: -5.5; -4,2) for day 14 and -12.4 (95%CI: -13.0; 11.8) for day 21 (Sidak test)) (Figure 1 A-B) and significantly increased ALP activity compared to control (2-way ANOVA $p < 0.0001$ for interaction between time and *Frzb* overexpression – $p < 0.05$ between control and overexpression at day 1, 7, 14 and 21, with difference between means respectively -3.2 (95%CI: -6.0;-0.5) for day 1, -9.9 (95%CI: -12.6;-7.1) for day 7, -14.2 (95%CI: -16.9;-11.4) for day 14 and -7.3 (95%CI: -10.0;-4.5) for day 21 (Sidak test)) (Figure 1 C). Similar results were obtained with two additional and independent clones. Treatment of control MC3T3-E1 cells with conditioned medium (CM) from *Frzb* overexpressing cells increased both Alizarin Red staining (unpaired t-test p=0.007) (Figure 1 D-E) and ALP activity (unpaired t-test p=0.03) (Figure 1 F) at day 21.

Overexpression of *Frzb* modulates Wnt signaling and osteogenic differentiation

SFRPs were originally identified as inhibitors of Wnt signaling. Overexpression of *Frzb* decreased both active and total β-catenin. In contrast, *Frzb* overexpression increased the total amount and phosphorylation of CamKII and phosphorylated CREB, which is a downstream target of CamKII (Figure 2 A). This suggests a negative effect on canonical signaling, but a positive effect on the non-canonical Wnt/Ca2+ pathway.

Frzb overexpression decreased levels of *Axin2*, a known target gene in the canonical Wnt cascade (2-way ANOVA $p = 0.0029$ for interaction between time and *Frzb* overexpression – $p < 0.05$ between control and overexpression at day 14 and 21, with difference between means respectively 36.7 (95%CI: 19.3; 54.0) for day 14 and 28.9 (95%CI: 11.5; 46.2) for day 21 (Sidak test)) (Figure 2 B). Gain of Frzb increased expression of osteoblast-specific transcription factors *Osterix* (2-way ANOVA $p < 0.0001$ for interaction between time and *Frzb* overexpression – $p < 0.05$ between control and overexpression at day 7, 14 and 21, with difference between means respectively -446.5 (95%CI: -658.5; -234.6) for day 7, -899.0 (95%CI: -1111; -687.1) for day 14 and -624.5 (95%CI: -836.4; -412.6) for day 21 (Sidak test)) and *Osteocalcin* (2-way ANOVA $p < 0.0001$ for interaction between time and *Frzb* overexpression – $p < 0.05$ between control and overexpression at day 14 and 21, with difference between means respectively -12364 (95%CI: -16444;-8284) for day 14 and -52075 (95%CI: -56155;-47995) for day 21 (Sidak test)) (Figure 2 B). Similar data were obtained in two additional experiments and for two other, independent cell lines overexpressing *Frzb*..

Loss of Frzb negatively affects osteogenesis

Silencing of endogenous *Frzb* throughout the 21-day experiment was obtained by a pGIPZ-shRNAmir plasmid directed against *Frzb* (32%, 47%, 95% and 97% knockdown at day 1, 7, 14 and 21). Loss of *Frzb* decreased Alizarin red staining at day 14 and day 21 (2-way ANOVA $p = 0.02$ for interaction between time and *Frzb* silencing – $p < 0.05$ between control and silencing at day 14 and 21, with difference between means respectively 0.6637 (95%CI: 0.1; 1.2) for day 14 and 0.8520 (95%CI:0.3; 1.4) for day 21 (Sidak test)) (Figure 3 A-B) and reduced ALP activity (2-way ANOVA $p <0.0001$ for interaction between time and *Frzb* silencing – $p < 0.05$ between control and silencing at day 14 and 21, with difference between means respectively 3.6 (95%CI: 3.3;3.9) for day 14 and 8.358 (95%CI:8.0;8.7) for day 21 (Sidak test)) (Figure 3 C) compared to control shRNAmir. Decreased *Frzb* levels showed a reverse effect compared to overexpression on canonical and non-canocial cascades (Figure 3 D). Loss of *Frzb* reduced expression of *Osterix* (2-way ANOVA $p < 0.0001$ for interaction between time and *Frzb* silencing – $p <$

0.05 between control and silencing at day 14 and 21, with difference between means respectively 13.7 (95%CI: 9.4; 17.9) for day 14 and 18.2 (95%CI: 13.9; 22.4) for day 21 (Sidak test)) and *Osteocalcin* (2-way ANOVA $p < 0.0001$ for interaction between time and *Frzb* silencing – $p < 0.05$ between control and silencing at day 21, with difference between means respectively 412.3 (95%CI: 346.0;478.6) for day 21 (Sidak test)), but did not affect *Axin2* expression (Figure 3 E). Similar data were obtained in an additional experiment and for an other, independent cell line with loss of *Frzb*..

Validation in primary human periosteal cells (hPDCs) and human bone marrow stromal cells (hBMSCs)

To translationally validate the positive effects of FRZB on primary human cells, we used hPDCs and hBMSCs, cell types with strong osteogenic potential. Treatment of hPDCs and hBMSCs with CM from MC3T3-E1 cells overexpressing *Frzb* increased Alizarin red staining at day 28 (unpaired t-test p=0.03 and p=0.02) (Figure 4).

$Frzb_{NTN}$ overexpression mimics full length Frzb overexpression in osteogenesis

We further studied the effect of the CRD domain and NTN motif in our assays. Sustained high expression of the $Frzb_{NTN}$ domain (average fold increase compared to control $3.1*10^3$) increased Alizarin red staining (2-way ANOVA $p < 0.0001$ for interaction between time and *Frzb* overexpression – $p < 0.05$ between control and overexpression at day 14 and 21, with difference between means respectively -10.6 (95%CI: -11.8; -9.3) for day 14 and -25.5 (95%CI: -26.8; -24.2) for day 21 (Sidak test)) (Figure 5 A,C) and ALP activity (2-way ANOVA $p < 0.0001$ for interaction between time and *Frzb* overexpression – $p < 0.05$ between control and overexpression at day 1, 7, 14 and 21, with difference between means respectively -2.1 (95%CI: -2.8; -1.5) for day 1, -3.9 (95%CI: -4.5; -3.3) for day 7, -4.3 (95%CI: -4.9; -3.7) for day 14 and -9.6 (95%CI: -10.2;-9.0) for day 21 (Sidak test)) (Figure 5 D). Additionally, gain of $Frzb_{NTN}$ increased *Osterix* expression at day 7 (2-way ANOVA $p = 0.04$ for interaction between time and *Frzb* overexpression – $p < 0.05$ between control and overexpression at day 7 with difference between means

respectively -132.0 (95%CI: -233.6; -30.5) for day 7 (Sidak test)) (Figure 5 E). Similar data were obtained in two additional experiments and for two other, independent cell lines overexpressing $Frzb_{NTN}$. Treatment of hBMSCs with CM from MC3T3-E1 cells overexpressing $Frzb_{NTN}$ increased Alizarin red staining at day 28 (unpaired t-test p=0.01) (Figure 5 B). On the contrary, overexpression of the $Frzb_{CRD}$ (average fold increase compared to control 75) domain slightly decreased Alizarin red staining (2-way ANOVA $p = 0.0007$ for interaction between time and *Frzb* overexpression – $p < 0.05$ between control and overexpression at day 7 and 21, with difference between means respectively 0.2 (95%CI: 0.09; 0.3) for day 7 and 0.1 (95%CI: 0.0002;0.2) for day 21 (Sidak test)) (Figure 5 F,H) and ALP activity (2-way ANOVA $p < 0.0001$ for interaction between time and *Frzb* overexpression – $p < 0.05$ between control and overexpression at day 14 and 21, with difference between means respectively 7.0 (95%CI: 6.1;7.9) for day 14 and 5.2 (95%CI: 4.3;6.1) for day 21 (Sidak test)) (Figure 5 I). Moreover, the $Frzb_{CRD}$ domain did not consistently alter *Osterix* expression (Figure 5 J). Similar data were obtained in two additional experiments and for two other, independent cell lines overexpressing $Frzb_{CRD}$. $Frzb_{NTN}$ overexpression decreased active β-catenin and increased phosphorylated CamKII at day 21, while $Frzb_{CRD}$ overexpression decreased both active and total β-catenin throughout the whole experiment and decreased phosphorylated CamKII at day 21 (Figure 6 A-B). Treatment of hBMSCs with CM from MC3T3-E1 cells overexpressing $Frzb_{CRD}$ decreased Alizarin red staining at day 28 (unpaired t-test p<0.0001) (Figure 5 G).

Interaction of FrzbNTN and FrzbCRD with full length Frzb and Wnts

The observations reported above could indicate that $Frzb_{NTN}$ and $Frzb_{CRD}$ have a dominant-negative effect on the full-length protein. To further investigate potential competition of the overexpressed domains with the full length protein, we treated MC3T3-E1 cells control cells and cells overexpressing $Frzb_{NTN}$ or $Frzb_{CRD}$ with recombinant mFrzb for 14 days. Adding recombinant FRZB to the differentiation culture slightly but significantly increased Alizarin Red staining in $Frzb_{NTN}$ overexpressing cells without a similar increase in ALP activity. In contrast, we did not detect a difference in Alizarin Red staining and ALP

activity for control and $Frzb_{CRD}$ overexpressing cells after treatment with recombinant FRZB (Supplementary Figure 1A-C).

Next, we also studied the interactions between exogenously added Wnts and FRZB overexpressing cells. Wnt3a decreased Alizarin red staining in cells overexpressing Frzb and $Frzb_{NTN}$+ and decreased ALP activity in control cells and overexpressing Frzb. For Wnt5a, we could observe a decrease in Alizarin red staining for cells overexpressing Frzb, but we detected no differences in ALP activity (Supplementary Figure 2A-C). Moreover, treatment of MC3T3-E1 with recombinant mWnt3a resulted in an increase in active beta-catenin and phosphorylated CamKII in cells overexpressing Frzb and $Frzb_{NTN}$, but in a decrease in canonical Wnt signaling in control cells. Addition of recombinant mWnt5a only positively influenced canonical Wnt signaling in cells overexpressing Frzb (Supplementary Figure 2 D)..

DISCUSSION

In our experiments, *Frzb* overexpression *in vitro* stimulated osteogenesis and was associated with reduced canonical and increased non-canonical Wnt signaling. On the other hand, loss of Frzb decreased osteogenesis. This observed positive effect on osteogenesis appears in line with earlier *in vitro* data suggesting that recombinant Frzb increased osteoblast differentiation (15). However, these and our results appear contradictory to *in vivo* data showing that $Frzb^{-/-}$ mice have increased cortical bone thickness (10) but not trabecular bone thickness and with the well-known observation that excess of Wnt signaling results in high bone mass phenotypes in mice and men (16-21). Other Wnt antagonists have also been shown to negatively affect bone formation. Genetic deletion of Sfrp1 in mice leads to an increased trabecular bone, while overexpression of SFRP1 inhibits bone formation (22-24). Furthermore, Sfrp1 acts as a negative regulator of human osteoblast and osteocyte survival and may also inhibit osteoclastogenesis by a Wnt-independent mechanism (22). Sfrp4 also negatively affects bone formation and SFRP4 was also

proposed to be involved in phosphate metabolism, but others could not confirm this link (25, 26). Additionally, loss of sclerostin (SOST) expression in bone was found to result in Van Buchem disease (27). In mice, targeted deletion of Sost results in increased bone formation and strength, while mice overexpressing *Sost* have low bone mass and decreased bone strength (28-30). Another Wnt antagonist, DKK1, regulates bone mass with increased expression linked to osteopenia and decreased expression associated with HBM (31). *Dkk1* knockout mice are embryonic lethal, however, an allelic series of mice with decreased DKK1 expression levels ($Dkk1^{+/+}$, $Dkk1^{+/d}$, $Dkk1^{+/-}$ and $Dkk1^{d/-}$) show that for both the trabecular and the cortical bone, bone mass is inversely proportional to the level of DKK1 (31). Interestingly, Dkk2, like Frzb, positively influences the formation of mineralized matrix in the late stages of osteogenic differentiation and this effect might not be entirely mediated by its Wnt signaling antagonistic activity (32). We hypothesize that this surprising contrast between *in vitro* and *in vivo* observations can be explained by the high and therefore supraphysiological levels of the Wnt modulator. This overexpression may affect the protein's biological effects in different ways. Moreover, high local concentrations may be achieved *in vivo* in specific compartments of the skeleton but more importantly could be the goal of a treatment strategy. Frzb expression levels significantly increase during osteogenesis of MC3T3-E1 cells (Supplementary Figure 3), suggesting that Frzb plays an important role in the later stages of osteogenesis and mineralisation. This is in line with the expression profile of Dkk1, Dkk2, Sclerostin and SFRP1, also Wnt inhibitors, during osteogenic differentiation (22, 32-34). Interestingly, while Sfrp1, Dkk1 and Sclerostin inhibit osteogenesis Dkk2 overexpression shows a similar effect as Frzb (33, 34).

Excess of canonical Wnt signaling results typically in high bone mass phenotypes in mice and men (16-21). However, in our gain of function studies, we observed a decrease in canonical Wnt signaling together with augmented osteogenesis and activation of the non-canonical Wnt/CamKII pathway. Although the effects of FRZB on osteogenesis can be mediated in part by its Wnt-inhibiting effect, we consider that the

role of FRZB in osteoblast differentiation is not limited to its Wnt-antagonistic effect. First, our data suggest that canonical Wnt signaling is not the only mediator to drive osteogenesis in this *in vitro* system. The increase of osteogenesis could, at least partly, be caused by an increase of non-canonical Wnt signaling. Ca^{2+} signaling and Ca^{2+} transport play key roles during osteoblast differentiation and bone formation. Many of the cellular effects of Ca^{2+} are mediated by the Ca^{2+} binding protein, Calmodulin (CaM). Activation of CaM activates in turn both CamKII and CaN (35). Zayzafoon et al. showed that inhibition of αCamKII results in a decrease in osteoblast differentiation (36). Additionally, CamKII can stimulate osteoblastogenesis by modulating the activity of Osterix, a transcription factor essential for osteoblast differentiation and bone mineralization, and Dlx5, that mediates the transcriptional control by many osteoblastogenic signaling pathways (37, 38).

Secondly, although SFRPs were originally identified as soluble Wnt inhibitors that bind directly to Wnts and prevent their interaction with Fz receptors. However, different biochemical and crystallographic data suggested that SFRPs could both activate and inactivate Wnt signaling. SFRPs and Fz receptors have been shown to form homodimers and heterodimers via their CRD domains and subsequently stimulate signal transduction (7). In our experimental setting *Frzb* overexpression inhibited canonical Wnt signaling, but stimulated non-canonical Wnt/Ca2+ signaling, by increasing both phosphorylated and total CamKII. Direct effects of modulator-receptor interaction therefore provide a possible explanation for our observations and require further research. Of note, Nalesso et al. demonstrated that distinct Wnt pathways are reciprocally inhibitory and in equilibrium and therefore selective inhibition of the canonical pathway enhances the activation of the Ca^{2+} mobilization (39). SFRPs have different binding affinities for distinct Wnt ligands (40). Canonical and noncanonical signaling pathway activation involves the shared use of the same Fz receptors. Therefore, excess of either type of Wnt might interfere with the other pathway as a result of ligand competition for binding to Fz (41). Thirdly, SFRPs can interfere with protease activity

(42), interact with proteins which are not directly involved in the Wnt signaling cascade and affect BMP signaling (7, 42-45).

Frzb$_{NTN}$ overexpression induced similar effects on osteogenesis as full length *Frzb*, whereas *Frzb*$_{CRD}$ overexpressing cells mimicked loss of *Frzb* experiments. The CRD domain of Sfrps is considered the Wnt binding domain and is therefore most studied. Nevertheless, our data indicate that the NTN domain can also have strong effects on bone differentiation. Both the CRD and NTN domain are required for Wnt binding in Drosophila (9). We cannot exclude that the NTN domain has a role in Wnt binding. Earlier work found SNPs in the NTN domain associated with hip osteoarthritis (46). Additional data in this paper demonstrated that these variants in the NTN domain resulted in reduced Wnt antagonistic activity for the full length molecule. In addition, Wnt-binding may not fully explain the observation that overexpression of Frzb$_{NTN}$ or Frzb$_{CRD}$ resulted in a different outcome. The NTN domain shows sequence similarity to Netrin, TIMPs and PCOLCEs. In TIMPs and PCOLCEs, the NTN domain is thought to interfere with protease activity. The Sfrp$_{NTN}$ domain may also have protease inhibitory activity (47). For example, SFRP2 can act as a procollagen C proteinase enhancer of Tolloid-like metalloproteinases in myocardial infarction-associated fibrosis (48), SFRP1 can act as an inhibitor of the A Disintegrin and metalloproteinase domain-containing protein 10 metalloprotease (49), Sizzled, a non-mammalian Sfrp family member, stabilizes Chordin by binding and inhibiting the Tolloid-family metalloproteinase, Bmp1a (43). Thus, even in a relatively straightforward *in vitro* setting FRZB and other SFRPs may have more complex biological effects than anticipated upon their discovery and initial functional assessment.

Although the use of stable cell lines is interesting from a practical point of view, this approach also has limitations. The exposure of the cells through their expansion to high levels of FRZB or modified forms of the molecule may affect their behavior in the described experiments. We also tested whether the mutated forms would have dominant-negative effects and how they interact with Wnt ligands. However, adding FRZB to FRZB$_{NTN}$ overexpressing cells has a small but significant positive effect and not a

competitive effect on osteogenesis. Wnt3a and Wnt5a do not seem to be able to interact with CRD domain without the NTN domain. However, FRZB and the $FRZB_{NTN}$ appear to antagonize the inhibitory effect of Wnt3a on osteogenic differentiation.

In summary, our observation that overexpression of *Frzb* promotes bone differentiation and shifts balances between Wnt signaling cascades provides novel perspectives on the Wnt signaling pathway as a therapeutic target for bone and joint diseases. SFRPs or their specific domains may hold potential as therapeutics taking into account that our strong gain and loss of function approaches highlight that excess of SFRPs has effects that are not expected under physiological, endogenous expression conditions.

ACKNOWLEDGEMENTS

S.T., F.C, R.L designed the project and wrote the manuscript. S.T. performed the experiments. S.T., F.C. and R.L. analyzed the data.

Supplementary Information accompanies the paper on the Laboratory Investigation website (http://www.nature.com/labinvest).

DISCLOSURE

The authors state to have no duality of interest to declare.

LIST OF ABBREVIATIONS

alkaline phosphatase (ALP); calcium-calmodulin-dependent kinase II (CamKII); conditioned medium (CM); cysteine-rich domain (CRD); Frizzled (Fz); Frizzled related protein (FRZB); hypoxanthine guanine phosphoribosyl transferase1(Hprt1); human periosteum-derived cells (hPDCs); Netrin-like (NTN); secreted frizzled related protein (SFRP)

REFERENCES

1. Westendorf JJ, Kahler RA, Schroeder TM. Wnt signaling in osteoblasts and bone diseases. Gene. 2004;341:19-39.

2. Baron R, Kneissel M. WNT signaling in bone homeostasis and disease: from human mutations to treatments. Nat Med. 2013;19(2):179-92.

3. Clevers H, Nusse R. Wnt/beta-catenin signaling and disease. Cell. 2012;149(6):1192-205.

4. MacDonald BT, Tamai K, He X. Wnt/beta-catenin signaling: components, mechanisms, and diseases. Dev Cell. 2009;17(1):9-26.

5. Gao C, Chen YG. Dishevelled: The hub of Wnt signaling. Cell Signal. 2010;22(5):717-27.

6. Cruciat CM, Niehrs C. Secreted and transmembrane wnt inhibitors and activators. Cold Spring Harb Perspect Biol. 2013;5(3):a015081.

7. Bovolenta P, Esteve P, Ruiz JM, Cisneros E, Lopez-Rios J. Beyond Wnt inhibition: new functions of secreted Frizzled-related proteins in development and disease. J Cell Sci. 2008;121(Pt 6):737-46.

8. Gorny AK, Kaufmann LT, Swain RK, Steinbeisser H. A secreted splice variant of the Xenopus frizzled-4 receptor is a biphasic modulator of Wnt signalling. Cell Commun Signal. 2013;11:89.

9. Uren A, Reichsman F, Anest V, Taylor WG, Muraiso K, Bottaro DP, et al. Secreted frizzled-related protein-1 binds directly to Wingless and is a biphasic modulator of Wnt signaling. J Biol Chem. 2000;275(6):4374-82.

10. Lories RJ, Peeters J, Bakker A, Tylzanowski P, Derese I, Schrooten J, et al. Articular cartilage and biomechanical properties of the long bones in Frzb-knockout mice. Arthritis Rheum. 2007;56(12):4095-103.

11. Lin K, Wang S, Julius MA, Kitajewski J, Moos M, Jr., Luyten FP. The cysteine-rich frizzled domain of Frzb-1 is required and sufficient for modulation of Wnt signaling. Proc Natl Acad Sci U S A. 1997;94(21):11196-200.

12. De Bari C, Dell'Accio F, Luyten FP. Human periosteum-derived cells maintain phenotypic stability and chondrogenic potential throughout expansion regardless of donor age. Arthritis Rheum. 2001;44(1):85-95.

13. Roobrouck VD, Clavel C, Jacobs SA, Ulloa-Montoya F, Crippa S, Sohni A, et al. Differentiation potential of human postnatal mesenchymal stem cells, mesoangioblasts, and multipotent adult progenitor cells reflected in their transcriptome and partially influenced by the culture conditions. Stem Cells. 2011;29(5):871-82.

14. Giulietti A, Overbergh L, Valckx D, Decallonne B, Bouillon R, Mathieu C. An overview of real-time quantitative PCR: applications to quantify cytokine gene expression. Methods. 2001;25(4):386-401.

15. Chung YS, Baylink DJ, Srivastava AK, Amaar Y, Tapia B, Kasukawa Y, et al. Effects of secreted frizzled-related protein 3 on osteoblasts in vitro. J Bone Miner Res. 2004;19(9):1395-402.

16. Boyden LM, Mao J, Belsky J, Mitzner L, Farhi A, Mitnick MA, et al. High bone density due to a mutation in LDL-receptor-related protein 5. N Engl J Med. 2002;346(20):1513-21.

17. Little RD, Carulli JP, Del Mastro RG, Dupuis J, Osborne M, Folz C, et al. A mutation in the LDL receptor-related protein 5 gene results in the autosomal dominant high-bone-mass trait. Am J Hum Genet. 2002;70(1):11-9.

18. Babij P, Zhao W, Small C, Kharode Y, Yaworsky PJ, Bouxsein ML, et al. High bone mass in mice expressing a mutant LRP5 gene. J Bone Miner Res. 2003;18(6):960-74.

19. Zhang Y, Wang Y, Li X, Zhang J, Mao J, Li Z, et al. The LRP5 high-bone-mass G171V mutation disrupts LRP5 interaction with Mesd. Mol Cell Biol. 2004;24(11):4677-84.

20. Semenov MV, He X. LRP5 mutations linked to high bone mass diseases cause reduced LRP5 binding and inhibition by SOST. J Biol Chem. 2006;281(50):38276-84.

21. Balemans W, Devogelaer JP, Cleiren E, Piters E, Caussin E, Van Hul W. Novel LRP5 missense mutation in a patient with a high bone mass phenotype results in decreased DKK1-mediated inhibition of Wnt signaling. J Bone Miner Res. 2007;22(5):708-16.

22. Bodine PV, Billiard J, Moran RA, Ponce-de-Leon H, McLarney S, Mangine A, et al. The Wnt antagonist secreted frizzled-related protein-1 controls osteoblast and osteocyte apoptosis. J Cell Biochem. 2005;96(6):1212-30.

23. Yao W, Cheng Z, Shahnazari M, Dai W, Johnson ML, Lane NE. Overexpression of secreted frizzled-related protein 1 inhibits bone formation and attenuates parathyroid hormone bone anabolic effects. J Bone Miner Res. 2010;25(2):190-9.

24. Bodine PV, Zhao W, Kharode YP, Bex FJ, Lambert AJ, Goad MB, et al. The Wnt antagonist secreted frizzled-related protein-1 is a negative regulator of trabecular bone formation in adult mice. Mol Endocrinol. 2004;18(5):1222-37.

25. Cho HY, Choi HJ, Sun HJ, Yang JY, An JH, Cho SW, et al. Transgenic mice overexpressing secreted frizzled-related proteins (sFRP)4 under the control of serum amyloid P promoter exhibit low bone mass but did not result in disturbed phosphate homeostasis. Bone. 2010;47(2):263-71.

26. Nakanishi R, Akiyama H, Kimura H, Otsuki B, Shimizu M, Tsuboyama T, et al. Osteoblast-targeted expression of Sfrp4 in mice results in low bone mass. J Bone Miner Res. 2008;23(2):271-7.

27. Uitterlinden AG, Arp PP, Paeper BW, Charmley P, Proll S, Rivadeneira F, et al. Polymorphisms in the sclerosteosis/van Buchem disease gene (SOST) region are associated with bone-mineral density in elderly whites. Am J Hum Genet. 2004;75(6):1032-45.

28. Collette NM, Genetos DC, Economides AN, Xie L, Shahnazari M, Yao W, et al. Targeted deletion of Sost distal enhancer increases bone formation and bone mass. Proc Natl Acad Sci U S A. 2012;109(35):14092-7.

29. Moester MJ, Papapoulos SE, Lowik CW, van Bezooijen RL. Sclerostin: current knowledge and future perspectives. Calcif Tissue Int. 2010;87(2):99-107.

30. Winkler DG, Sutherland MK, Geoghegan JC, Yu C, Hayes T, Skonier JE, et al. Osteocyte control of bone formation via sclerostin, a novel BMP antagonist. EMBO J. 2003;22(23):6267-76.

31. MacDonald BT, Joiner DM, Oyserman SM, Sharma P, Goldstein SA, He X, et al. Bone mass is inversely proportional to Dkk1 levels in mice. Bone. 2007;41(3):331-9.

32. Qiang YW, Barlogie B, Rudikoff S, Shaughnessy JD, Jr. Dkk1-induced inhibition of Wnt signaling in osteoblast differentiation is an underlying mechanism of bone loss in multiple myeloma. Bone. 2008;42(4):669-80.

33. Li X, Liu P, Liu W, Maye P, Zhang J, Zhang Y, et al. Dkk2 has a role in terminal osteoblast differentiation and mineralized matrix formation. Nat Genet. 2005;37(9):945-52.

34. Li X, Zhang Y, Kang H, Liu W, Liu P, Zhang J, et al. Sclerostin binds to LRP5/6 and antagonizes canonical Wnt signaling. J Biol Chem. 2005;280(20):19883-7.

35. Zayzafoon M. Calcium/calmodulin signaling controls osteoblast growth and differentiation. J Cell Biochem. 2006;97(1):56-70.

36. Zayzafoon M, Fulzele K, McDonald JM. Calmodulin and calmodulin-dependent kinase IIalpha regulate osteoblast differentiation by controlling c-fos expression. J Biol Chem. 2005;280(8):7049-59.

37. Seo JH, Jin YH, Jeong HM, Kim YJ, Jeong HG, Yeo CY, et al. Calmodulin-dependent kinase II regulates Dlx5 during osteoblast differentiation. Biochem Biophys Res Commun. 2009;384(1):100-4.

38. Choi YH, Choi JH, Oh JW, Lee KY. Calmodulin-dependent kinase II regulates osteoblast differentiation through regulation of Osterix. Biochem Biophys Res Commun. 2013;432(2):248-55.

39. Nalesso G, Sherwood J, Bertrand J, Pap T, Ramachandran M, De Bari C, et al. WNT-3A modulates articular chondrocyte phenotype by activating both canonical and noncanonical pathways. J Cell Biol. 2011;193(3):551-64.

40. Wawrzak D, Metioui M, Willems E, Hendrickx M, de Genst E, Leyns L. Wnt3a binds to several sFRPs in the nanomolar range. Biochem Biophys Res Commun. 2007;357(4):1119-23.

41. Grumolato L, Liu G, Mong P, Mudbhary R, Biswas R, Arroyave R, et al. Canonical and noncanonical Wnts use a common mechanism to activate completely unrelated coreceptors. Genes Dev. 2010;24(22):2517-30.

42. Lee HX, Ambrosio AL, Reversade B, De Robertis EM. Embryonic dorsal-ventral signaling: secreted frizzled-related proteins as inhibitors of tolloid proteinases. Cell. 2006;124(1):147-59.

43. Muraoka O, Shimizu T, Yabe T, Nojima H, Bae YK, Hashimoto H, et al. Sizzled controls dorso-ventral polarity by repressing cleavage of the Chordin protein. Nat Cell Biol. 2006;8(4):329-38.

44. Yabe T, Shimizu T, Muraoka O, Bae YK, Hirata T, Nojima H, et al. Ogon/Secreted Frizzled functions as a negative feedback regulator of Bmp signaling. Development. 2003;130(12):2705-16.

45. Misra K, Matise MP. A critical role for sFRP proteins in maintaining caudal neural tube closure in mice via inhibition of BMP signaling. Dev Biol. 2010;337(1):74-83.

46. Loughlin J, Dowling B, Chapman K, Marcelline L, Mustafa Z, Southam L, et al. Functional variants within the secreted frizzled-related protein 3 gene are associated with hip osteoarthritis in females. Proc Natl Acad Sci U S A. 2004;101(26):9757-62.

47. Chong JM, Uren A, Rubin JS, Speicher DW. Disulfide bond assignments of secreted Frizzled-related protein-1 provide insights about Frizzled homology and netrin modules. J Biol Chem. 2002;277(7):5134-44.

48. Kobayashi K, Luo M, Zhang Y, Wilkes DC, Ge G, Grieskamp T, et al. Secreted Frizzled-related protein 2 is a procollagen C proteinase enhancer with a role in fibrosis associated with myocardial infarction. Nat Cell Biol. 2009;11(1):46-55.

49. Esteve P, Sandonis A, Cardozo M, Malapeira J, Ibanez C, Crespo I, et al. SFRPs act as negative modulators of ADAM10 to regulate retinal neurogenesis. Nat Neurosci. 2011;14(5):562-9.

TITLES AND LEGENDS TO FIGURES

Figure 1: Overexpression of *Frzb* increases osteogenesis and this effect is induced by secreted factors. (A) Alizarin red (AR) staining of MC3T3-E1 cells overexpressing *Frzb* (Frzb+) compared to controls. (B) Quantification of the AR staining of 1 in 3 diluted samples. Data are expressed as relative absorbance compared control to cells at the same timepoint. (2-way ANOVA $p < 0.0001$ for interaction between time and *Frzb* overexpression – *$p < 0.05$ between control and overexpression) (C) Alkaline phosphatase (AP) activity of MC3T3-E1 cells overexpressing *Frzb* compared to controls. (2-way ANOVA $p < 0.0001$ for interaction between time and *Frzb* overexpression – *$p < 0.05$ between control and overexpression). Data (A-C) show mean±SD of three replicates, but similar data were obtained in two additional experiments and for two other, independent cell lines overexpressing Frzb.. MC3T3-E1 cells were stimulated with conditioned medium (CM) from *Frzb* overexpressing cells. (D) Alizarin red (AR) staining (E) Quantification of the AR staining. Data are expressed as the mean absorbance. Unpaired t-test *p=0.007. (F) Alkaline phosphatase activity. Unpaired t-test *p=0.03. Data presented (D-F) are representative of two independent experiments with CM and show mean±SD of three independent replicates.

Figure 2: Overexpression of Frzb stimulates osteogenesis by decreasing canonical but stimulating non-canonical signaling. Western blot analysis shows a decrease in active (dephosphorylated) β-catenin (92 kDa) and an increase in phosphorylated CamKII (50 kDa), total CamKII (50 kDa) and phosphorylated CREB (43 kDa) in *Frzb* (A) overexpressing cells. (B) mRNA expression levels of *Osterix* (2-way ANOVA $p < 0.0001$ for interaction between time and *Frzb* overexpression – *$p < 0.05$ between control and overexpression), *Osteocalcin* (2-way ANOVA $p < 0.0001$ for interaction between time and *Frzb* overexpression – *$p < 0.05$ between control and overexpression) and *Axin2* (2-way ANOVA $p = 0.0029$ for interaction between time and *Frzb* overexpression – *$p < 0.05$ between control and overexpression) in MC3T3-E1 cells stably overexpressing *Frzb* (Frzb+). All mRNA levels were normalized to *Hprt1*

(reference gene) and shown as relative expression levels compared to control (D1). Data (A-B) show mean±SD of three replicates, but similar data were obtained in two additional experiments and for two other, independent cell lines overexpressing Frzb..

Figure 3: Knockdown of *Frzb* reduces osteogenesis. (A) Alizarin red (AR) staining of MC3T3-E1 cells in which Frzb is stably knocked down ($Frzb_{KD}$) compared to controls. (B) Quantification of the AR staining. Data are expressed as relative absorbance compared to control cells at the same timepoint. (2-way ANOVA $p = 0.01$ for interaction between time and *Frzb* silencing – $*p < 0.05$ between control and silencing) (C) Alkaline phosphatase activity of $Frzb_{KD}$ cells compared to control at day 1. (2-way ANOVA $p < 0.0001$ for interaction between time and *Frzb* silencing – $*p < 0.05$ between control and overexpression).. (D) Western blot analysis shows a decrease in active (dephosphorylated) β-catenin (92 kDa) and increased phosphorylated CamKII (50 kDa) at day 14 (D14) and D21 in MC3T3-E1 cells in which Frzb is stably knocked down ($Frzb_{KD}$) compared to controls. (E) mRNA expression levels of *Osterix* (2-way ANOVA $p < 0.0001$ for interaction between time and *Frzb* silencing – $*p < 0.05$ between control and silencing), *Osteocalcin* (2-way ANOVA $p < 0.0001$ for interaction between time and *Frzb* silencing – $*p < 0.05$ between control and silencing)) and *Axin2* in $Frzb_{KD}$ cells with loss of Frzb. mRNA levels were normalized to Hprt1 (reference gene) and shown as relative expression levels compared to control (D1). Data (A-E) show mean±SD of three replicates, but similar data were obtained in two additional experiments and for two other, independent cell lines with loss of *Frzb*..

Figure 4: Positive effect of Frzb on osteogenesis in hPDCs and hBMSCs. (left) Alizarin red (AR) staining of hPDCs and hBMSCs treated with conditioned medium (CM) of MC3T3-E1 cells stably overexpressing the control or Frzb+ construct at day 28 (D28). (right) Quantification of the AR staining. Data are expressed as the percentage (%) of the area that is covered by mineralised nodules. Data are shown as mean±SD of three (hPDCs) or six (hBMSCs) independent replicates. Unpaired t-test *p=0.03 and *p=0.02.

Figure 5: $Frzb_{CRD}$ and $Frzb_{NTN}$ domain have different effects on osteogenesis. (A) Alizarin red (AR) staining of MC3T3-E1 cells with overexpressing $Frzb_{NTN}$ ($Frzb_{NTN}$+) compared to controls. (B) AR

staining of hBMSCs cells treated with conditionned medium (CM) of MC3T3-E1 cells stably overexpressing the control or $Frzb_{NTN}$+ construct at day 28 (D28) and quantification thereof. Data (B) are expressed as the percentage (%) of the area that is covered by mineralised nodules. Data are shown as mean±SD of six independent replicates. Unpaired t-test *p=0.01 (C) Quantification of the AR staining. Data are expressed as relative absorbance compared to control cells at the same timepoint. (2-way ANOVA $p < 0.0001$ for interaction between time and *Frzb* overexpression – $*p < 0.05$ between control and overexpression) (D) Alkaline phosphatase (AP) activity of $Frzb_{NTN}$+ cells compared to controls. (2-way ANOVA $*p < 0.0001$ for interaction between time and *Frzb* overexpression – $*p < 0.05$ between control and overexpression) (E) mRNA expression levels of *Osterix* at day 1 (D1) and D7. (2-way ANOVA $p = 0.0359$ for interaction between time and *Frzb* overexpression – $*p < 0.05$ between control and overexpression)) (F) AR staining of MC3T3-E1 cells overexpressing $Frzb_{CRD}$ ($Frzb_{CRD}$+) compared to controls. (G) AR staining of hBMSCs cells treated with conditionned medium (CM) of MC3T3-E1 cells stably overexpressing the control or $Frzb_{CRD}$+ construct at day 28 (D28) and quantification thereof. Data are expressed as the percentage (%) of the area that is covered by mineralised nodules. Data are shown as mean±SD of six independent replicates. Unpaired t-test *p<0.0001. (H) Quantification of the AR staining. (2-way ANOVA $p = 0.0007$ for interaction between time and *Frzb* overexpression – $*p < 0.05$ between control and overexpression)) (I) AP activity of $Frzb_{CRD}$+ cells compared to controls at different time points. (2-way ANOVA $p < 0.0001$ for interaction between time and *Frzb* overexpression – $*p < 0.05$ between control and overexpression)) (J) mRNA expression levels of *Osterix* at D1 and D7. mRNA levels were normalized to *Hprt1* (reference gene) and shown as relative expression levels compared to control (D1). Data (A, C-F, H-J) show mean±SD of three replicates, but similar data were obtained in two additional experiments and for two other, independent cell lines with loss of *Frzb*..

Figure 6: Both $Frzb_{CRD}$ and $Frzb_{NTN}$ overexpression decrease canonical Wnt signaling. (A) Western blot analysis shows a decrease in active (dephosphorylated) β-catenin (92 kDa) and a decrease in phosphorylated CamKII (50 kDa) in $Frzb_{NTN}$ overexpressing cells at day 21 (B) Western blot analysis

shows a decrease in active (dephosphorylated) β-catenin (92 kDa) and an increase in phosphorylated CamKII (50 kDa) in $Frzb_{CRD}$ overexpressing cells at day 21.

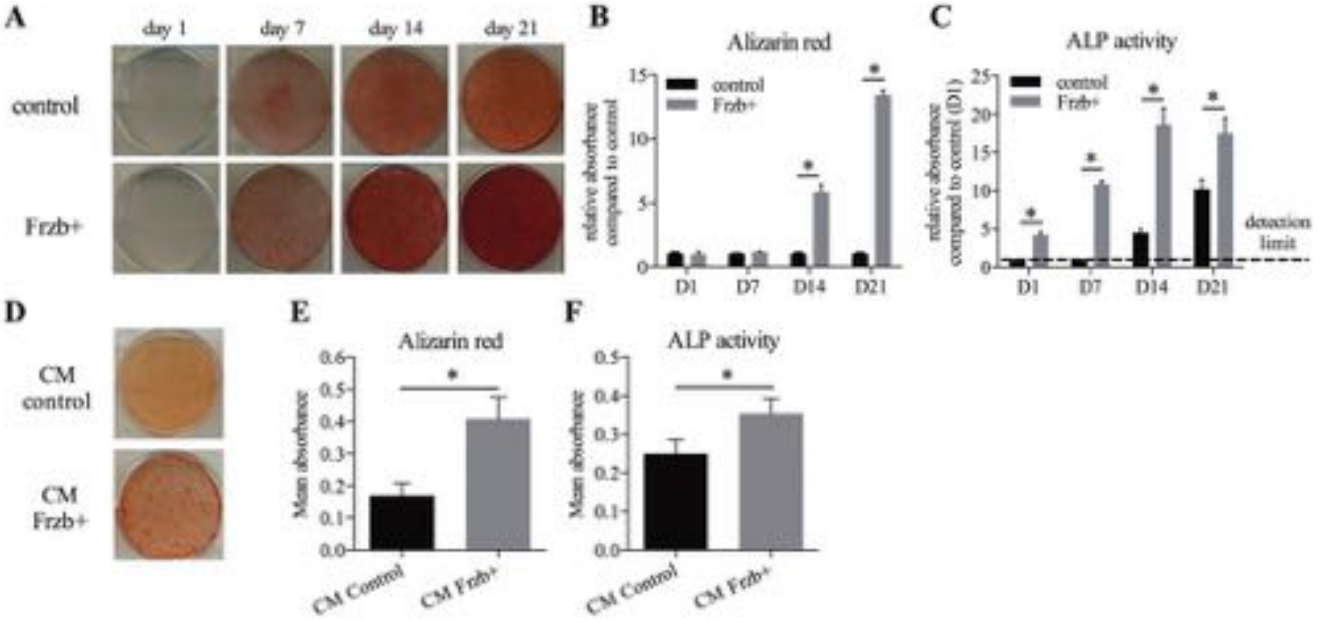
A
day 1
day 7
day 14
day 21
control
Frzb+
B
Alizarin red
control
Frzb+
relative absorbance compared to control
D1
D7
D14
D21
C
ALP activity
control
Frzb+
relative absorbance compared to control (D1)
detection limit
D1
D7
D14
D21
D
CM control
CM Frzb+
E
Alizarin red
Mean absorbance
CM Control
CM Frzb+
F
ALP activity
Mean absorbance
CM Control
CM Frzb+

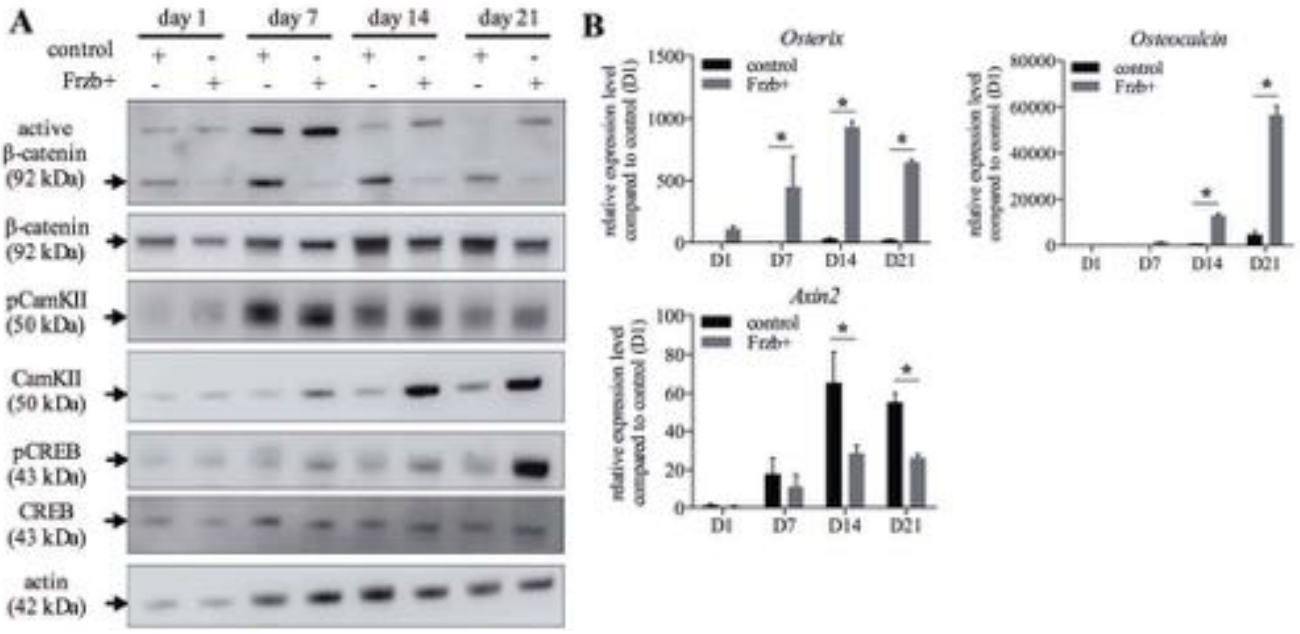
A
day 1
day 7
day 14
day 21
control
Frzb+
active β-catenin (92 kDa)
β-catenin (92 kDa)
pCamKII (50 kDa)
CamKII (50 kDa)
pCREB (43 kDa)
CREB (43 kDa)
actin (42 kDa)
B
Osterix
Osteocalcin
Axin2
control
Frzb+
relative expression level compared to control (D1)
D1
D7
D14
D21

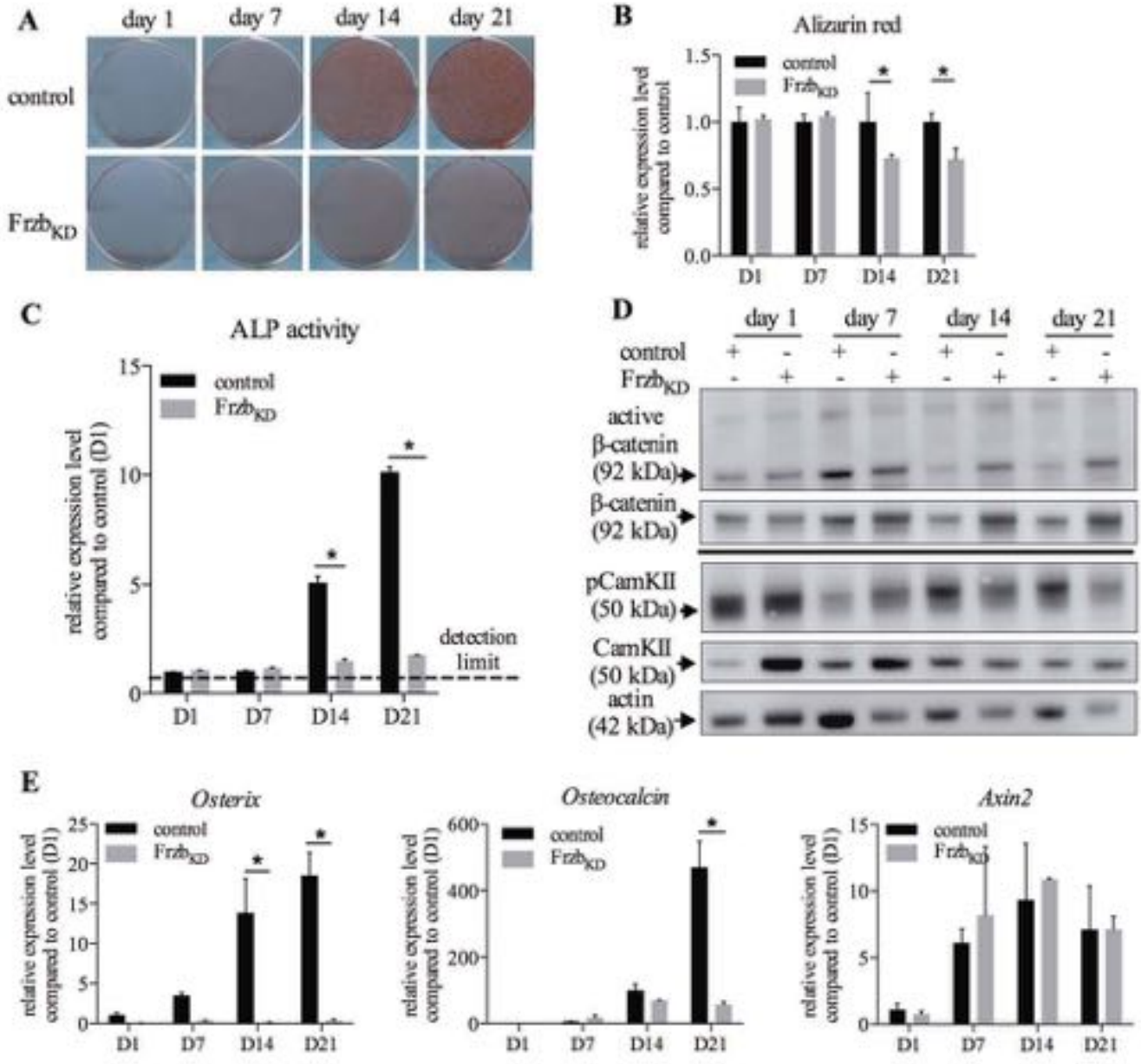
A
day 1
day 7
day 14
day 21
control
Frzb$_{KD}$
B
Alizarin red
relative expression level compared to control
control
Frzb$_{KD}$
1.5
1.0
0.5
0.0
D1
D7
D14
D21
C
ALP activity
relative expression level compared to control (D1)
control
Frzb$_{KD}$
15
10
5
0
detection limit
D1
D7
D14
D21
D
day 1
day 7
day 14
day 21
control
Frzb$_{KD}$
active β-catenin (92 kDa)
β-catenin (92 kDa)
pCamKII (50 kDa)
CamKII (50 kDa)
actin (42 kDa)
E
Osterix
Osteocalcin
Axin2
relative expression level compared to control (D1)
control
Frzb$_{KD}$
D1
D7
D14
D21

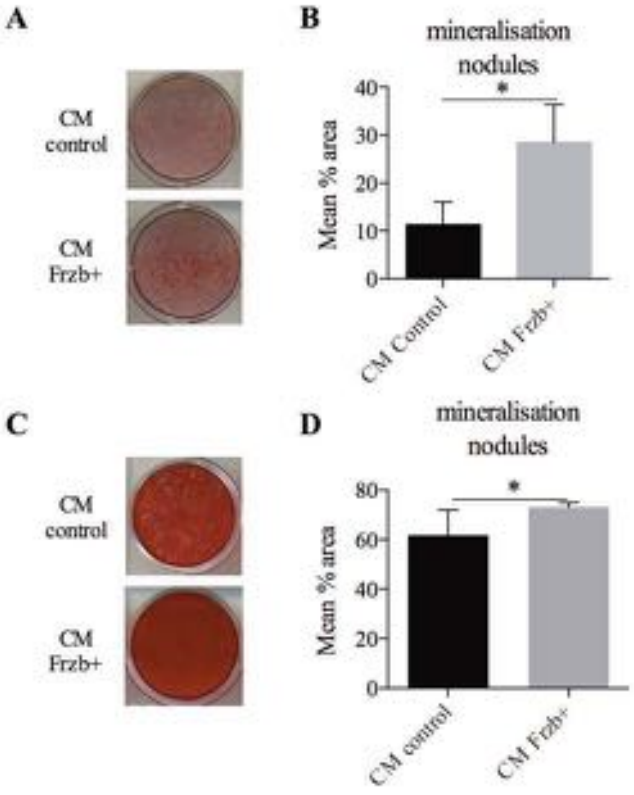
A
CM
control
CM
Frzb+
B
mineralisation
nodules
Mean % area
40
30
20
10
0
*
CM Control
CM Frzb+
C
CM
control
CM
Frzb+
D
mineralisation
nodules
Mean % area
80
60
40
20
0
*
CM control
CM Frzb+

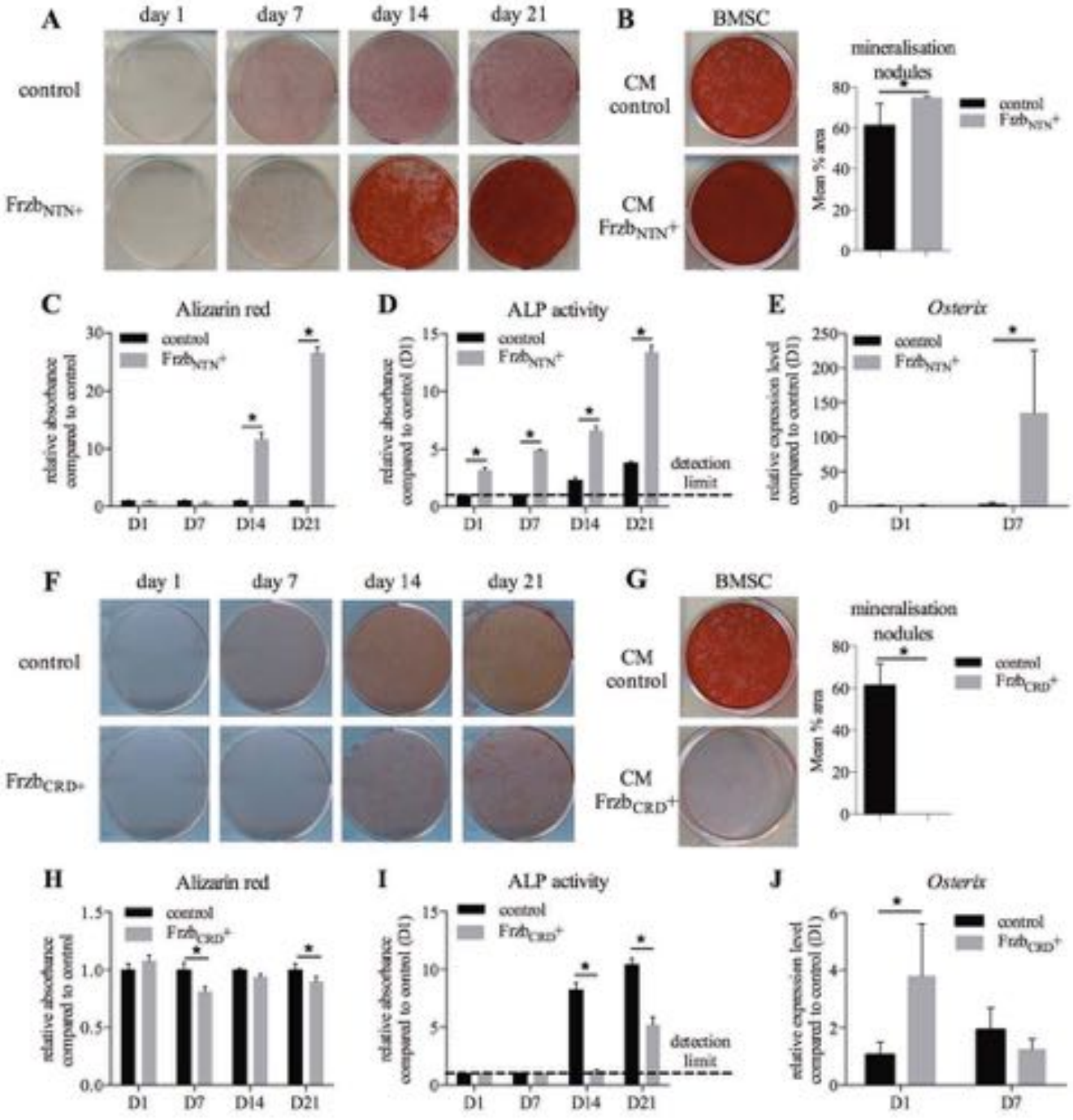
A
day 1
day 7
day 14
day 21
control
Frzb$_{NTN+}$
B
BMSC
CM control
CM Frzb$_{NTN+}$
mineralisation nodules
Mean % area
control
Frzb$_{NTN+}$
C
Alizarin red
relative absorbance compared to control
control
Frzb$_{NTN+}$
D1
D7
D14
D21
D
ALP activity
relative absorbance compared to control (D1)
detection limit
E
Osterix
relative expression level compared to control (D1)
F
control
Frzb$_{CRD+}$
G
CM control
CM Frzb$_{CRD+}$
mineralisation nodules
Frzb$_{CRD+}$
H
Alizarin red
I
ALP activity
J
Osterix

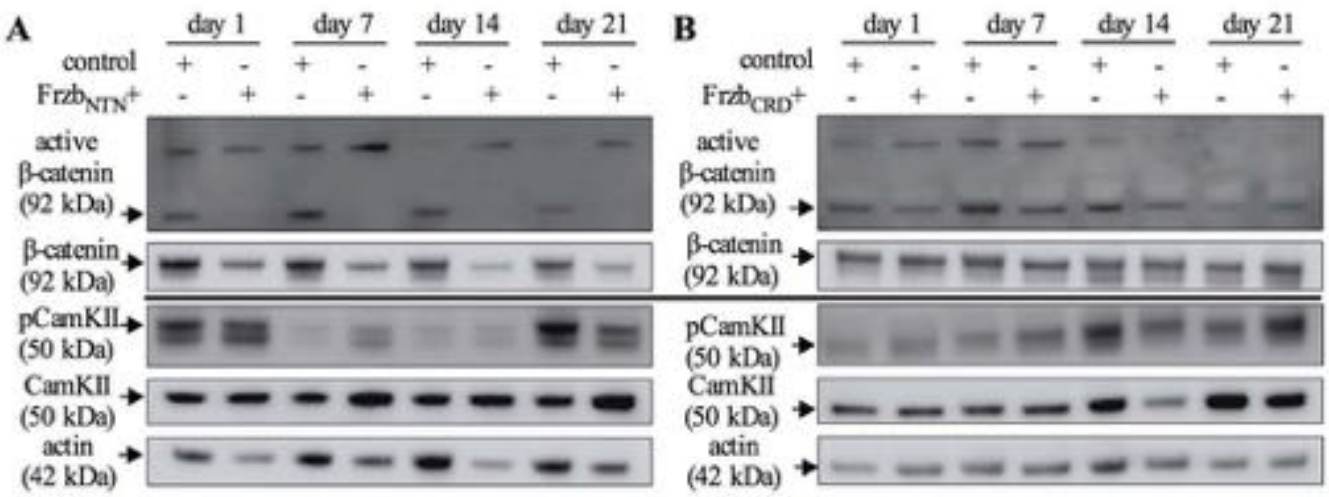
A
day 1
day 7
day 14
day 21
control
+ - + - + - + -
Frzb$_{NTN}$+
- + - + - + - +
active β-catenin (92 kDa)
β-catenin (92 kDa)
pCamKII (50 kDa)
CamKII (50 kDa)
actin (42 kDa)
B
day 1
day 7
day 14
day 21
control
+ - + - + - + -
Frzb$_{CRD}$+
- + - + - + - +
active β-catenin (92 kDa)
β-catenin (92 kDa)
pCamKII (50 kDa)
CamKII (50 kDa)
actin (42 kDa)

TABLES

Table 1. Primer sequences

	Forward primer (5'-3')	Reverse primer (5'-3')
bFrzb	GCATTCCCCTGTGCAAGT	GAGCAGTTCGAAGGTCTGCT
mFrzb	AGCCCTGCAAGTCTGTGTGT	CCCCTCTGCAGTGTCCAGTA
mOsterix	ATGGCGTCCTCTCTGCTTGA	AGTCCCGCAGAGGGCTAGAG
mOsteocalcin	AAGCAGGAGGGCAATAAGGT	CAGGGTTAAGCTCACACTGCTC
mAxin2	CCACCGCGAGTGTGAGAT	ACATAGCCGGAACCTACGTG
mHprt1	TGCTGACCTGCTGGATTACA	TAGTCAGTTGCCCCCTGTAT

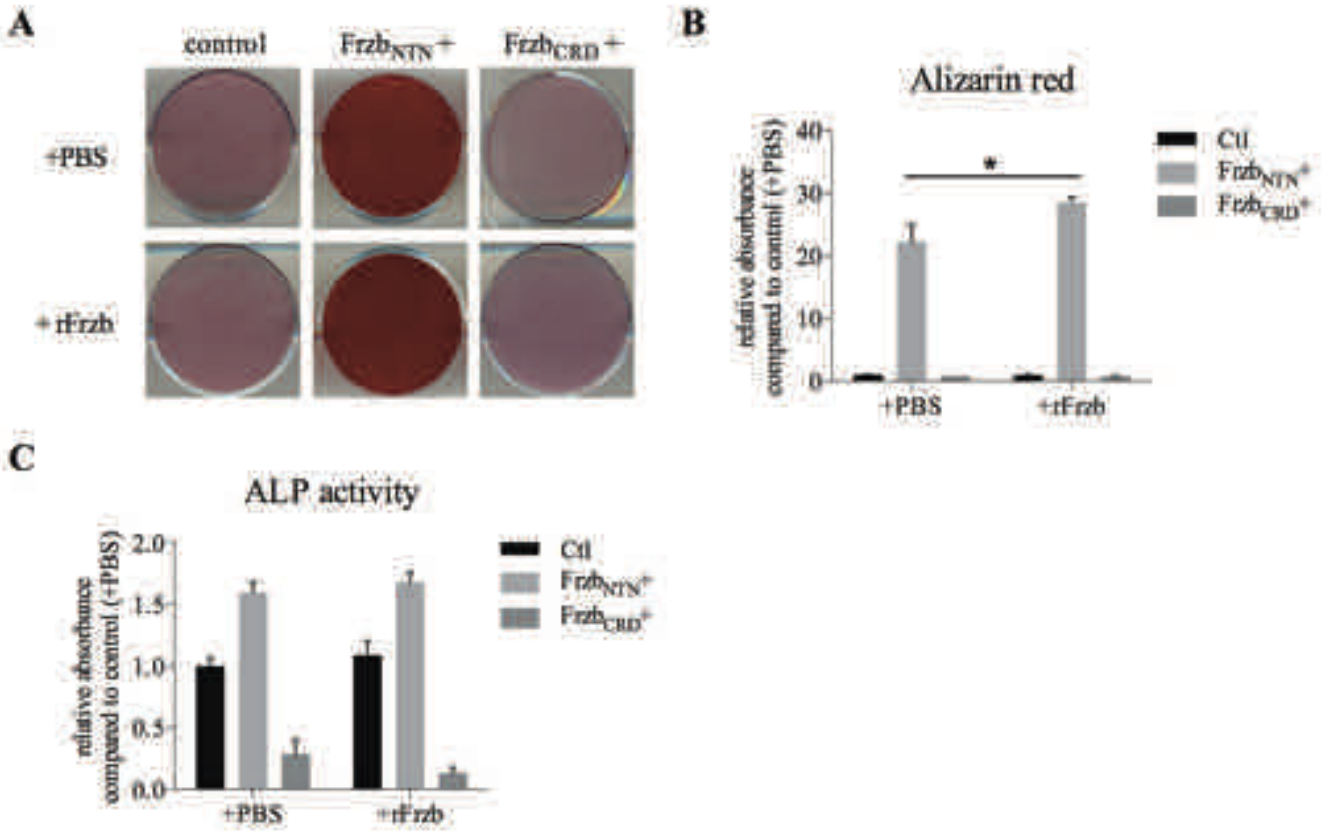
A
control
Frzb$_{NTN}$+
Frzb$_{CRD}$+
+PBS
+rFrzb
B
Alizarin red
relative absorbance compared to control (+PBS)
40
30
20
10
0
*
+PBS
+rFrzb
Ctl
Frzb$_{NTN}$+
Frzb$_{CRD}$+
C
ALP activity
relative absorbance compared to control (+PBS)
2.0
1.5
1.0
0.5
0.0
+PBS
+rFrzb
Ctl
Frzb$_{NTN}$+
Frzb$_{CRD}$+

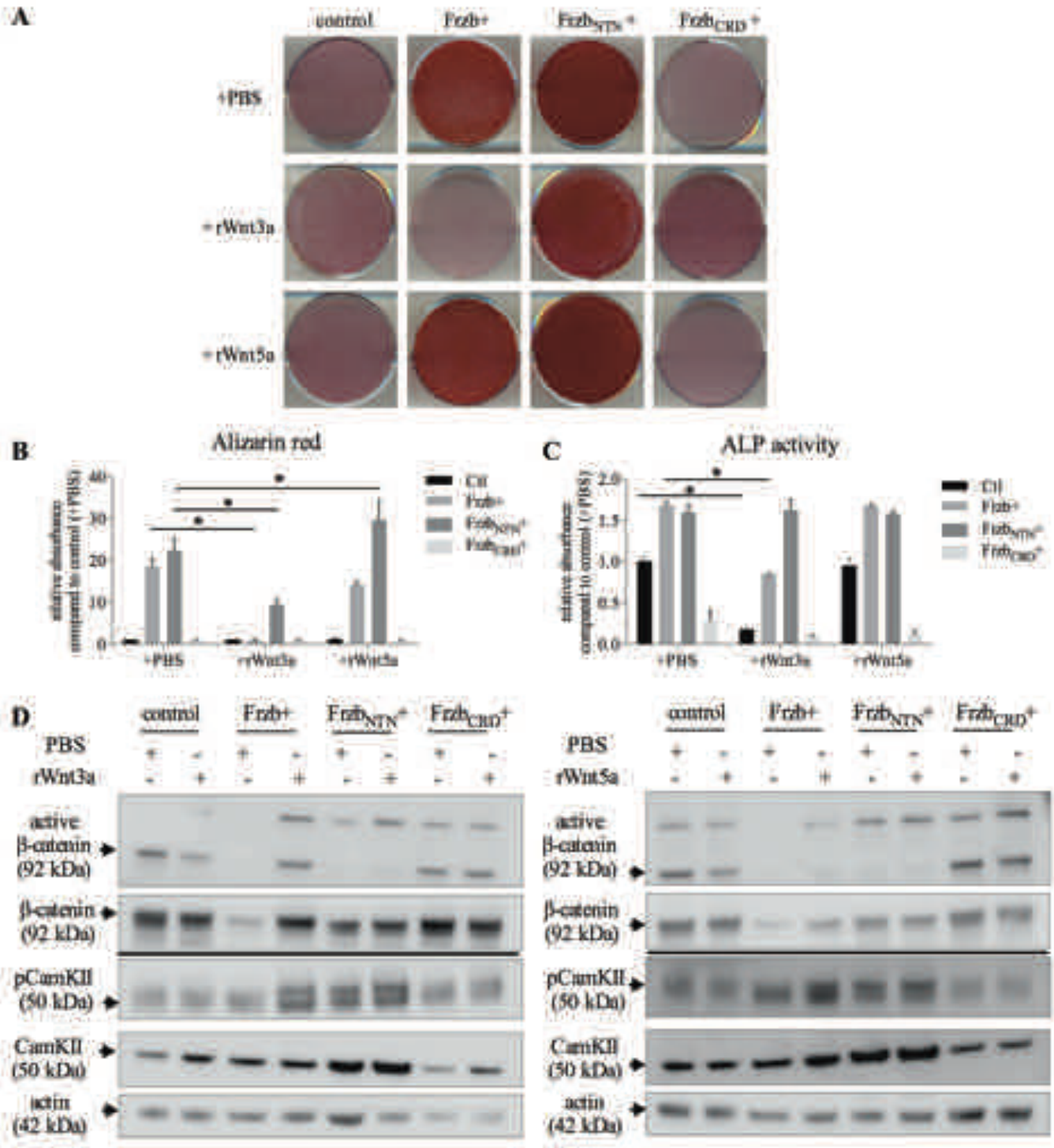
A
control
Frzb+
Frzb$_{NTN}$+
Frzb$_{CRD}$+
+PBS
+rWnt3a
+rWnt5a
B
Alizarin red
relative absorbance compared to control (+PBS)
Ctl
Frzb+
Frzb$_{NTN}$+
Frzb$_{CRD}$+
+PBS
+rWnt3a
+rWnt5a
C
ALP activity
relative absorbance compared to control (+PBS)
Ctl
Frzb+
Frzb$_{NTN}$+
Frzb$_{CRD}$+
+PBS
+rWnt3a
+rWnt5a
D
control
Frzb+
Frzb$_{NTN}$+
Frzb$_{CRD}$+
PBS
rWnt3a
active β-catenin (92 kDa)
β-catenin (92 kDa)
pCamKII (50 kDa)
CamKII (50 kDa)
actin (42 kDa)
control
Frzb+
Frzb$_{NTN}$+
Frzb$_{CRD}$+
PBS
rWnt5a
active β-catenin (92 kDa)
β-catenin (92 kDa)
pCamKII (50 kDa)
CamKII (50 kDa)
actin (42 kDa)

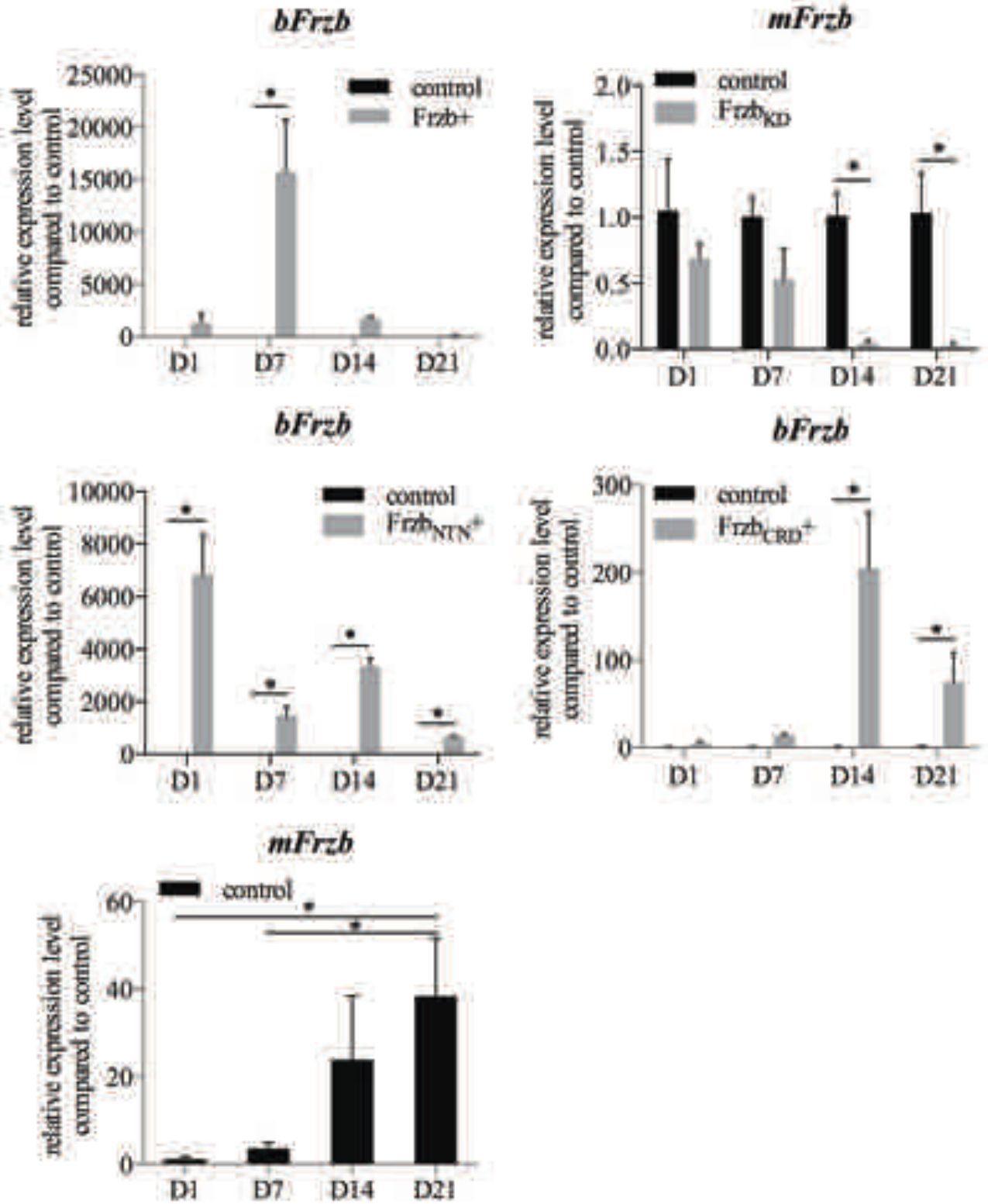
bFrzb
relative expression level compared to control
25000
20000
15000
10000
5000
0
control
Frzb+
D1
D7
D14
D21
mFrzb
2.0
1.5
1.0
0.5
0.0
control
Frzb_KD
bFrzb
10000
8000
6000
4000
2000
control
Frzb_NTN+
bFrzb
300
200
100
control
Frzb_CRD+
mFrzb
60
40
20
control